Mechanism of Alkyne Hydroarylation Catalyzed by (P,C)-Cyclometalated Au(III) Complexes

Marte Sofie Martinsen Holmsen,[†,a,b,c] Charlie Blons,[†,a] Abderrahmane Amgoune,[a] Matthieu Regnacq,[d] Denis Lesage,[d] E. Daiann Sosa Carrizo,[e] Pierre Lavedan,[f] Yves Gimbert,*[,d,g] Karinne Miqueu*[,e] and Didier Bourissou*[,a]

[†]These authors contributed equally.

*Emails: yves.gimbert@univ-grenoble-alpes.fr , karinne.miqueu@univ-pau.fr, didier.bourissou@univ-tlse3.fr

[a]CNRS/Université de Toulouse, UPS, Laboratoire Hétérochimie Fondamentale et Appliquée – LHFA UMR 5069, 118 route de Narbonne, 31062 Toulouse Cedex 09, France

[b]Centre for Materials Science and Nanotechnology, University of Oslo, P.O. Box 1126 Blindern, N-0316 Oslo, Norway

[c]Department of Chemistry, University of Oslo, P.O. Box 1033 Blindern, N-0315 Oslo, Norway

[d]CNRS/Sorbonne Université, Institut Parisien de Chimie Moléculaire – IPCM UMR 8232, 4 Place Jussieu, CC 229, 75252 Paris Cedex 05, France

[e]CNRS/Université de Pau et des Pays de l'Adour, E2S-UPPA, Institut des Sciences Analytiques et de Physico-Chimie pour l'Environnement et les Matériaux – IPREM UMR 5254. Hélioparc, 2 Avenue du Président Angot, 64053 Pau Cedex 09, France

[f]CNRS/Université de Toulouse, UPS, Institut de Chimie de Toulouse – ICT, 118 Route de Narbonne, 31062 Toulouse Cedex 09, France

[g]CNRS/Université Grenoble Alpes, UGA, Département de Chimie Moléculaire – DCM UMR 5250, 38000 Grenoble, France

Abstract: Over the last 5-10 years, gold(III) catalysis has developed rapidly. It often shows complementary if not unique features compared to gold(I) catalysis. While recent work has enabled major synthetic progress in terms of scope and efficiency, very little is yet known about the mechanism of Au(III)-catalyzed transformations and the relevant key intermediates have rarely been authenticated. Here we report a detailed experimental / computational mechanistic study of the recently reported intermolecular hydroarylation of alkynes catalyzed by (P,C)-cyclometalated Au(III) complexes. The cationic $(P,C)Au(OAc^F)^+$ complex ($OAc^F = OCOCF_3$) was authenticated by mass spectrometry (MS) in the gas phase and multi-nuclear NMR spectroscopy in solution at low temperature. According to DFT calculations, the OAc^F moiety is κ^2-coordinated to gold in the ground-state, but the corresponding κ^1-forms featuring a vacant coordination site sit only slightly higher in energy. Side-on coordination of the alkyne to Au(III) then promotes nucleophilic addition of the arene. The energy profiles for the reaction between trimethoxybenzene (TMB) and diphenylacetylene (DPA) were computed by DFT. The activation barrier is significantly lower for the outer-sphere pathway than for the alternative inner-sphere mechanism involving C–H activation of the arene followed by migratory insertion. The π-complex of DPA was characterized by MS. An unprecedented σ-arene Au(III) complex with TMB was also authenticated both in the gas phase and in solution. The cationic complexes $[(P,C)Au(OAc^F)]^+$ and $[(P,C)Au(OAc^F)(\sigma\text{-}TMB)]^+$ stand as active species and off-cycle resting state during catalysis, respectively. This study provides a rational basis for the further development of Au(III) catalysis based on π-activation.
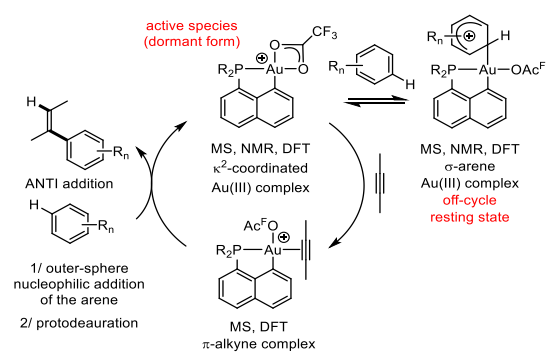
Introduction

Gold(III) chemistry and gold(III) catalysis have progressed spectacularly over the past decade and currently attract huge interest.[1] Au(III) complexes remain far less developed than Au(I) complexes in catalysis, but they are highly valuable synthetically, due to complementary properties and reactivity profiles.[2] A bottleneck in the development of gold(III) catalysts is certainly our limited knowledge about the associated reactivity and mechanistic intricacies. A few in-depth studies combining experiments and computations have recently unveiled the mechanism of some important Au(III)-catalyzed transformations such as the addition of trifluoroacetic acid to acetylene,[3] the alkoxycyclization of enynes[4] and the cyclopropanation of alkynes by propargyl esters.[5] Nonetheless, very few Au(III) intermediates relevant to catalysis have been authenticated experimentally and we are still far from having a comprehensive picture of Au(III) catalysis.

When it is to investigate experimentally the mechanism of Au(III)-catalyzed transformations, the subtle balance between stability and reactivity of Au(III) complexes constitutes a major hurdle. If chelating and cyclometalated ligands enable to prepare and handle 4-coordinate square-planar Au(III) complexes,[1b,6] the use of N and C-based ligands (pyridines, oxazolines, *N*-heterocyclic carbenes) is often mandatory and the presence of a vacant coordination site or labile ligand at Au(III) most often results in high instability due to fast reduction into Au(I) or Au(0) species.

Our group has shown P-based ligands with P^P/P^N chelating or P,C-cyclometalated frameworks to also be very powerful in stabilizing Au(III) complexes.[7] In particular, the (P,C)Au(III) complexes **1**, which are readily accessible by P-chelation assisted oxidative addition to gold,[8] proved very efficient in catalyzing the intermolecular hydroarylation of alkynes (Scheme 1).[9,10] Thanks to the labile OAc^F groups at gold (OAc^F = OCOCF$_3$),[11] the transformation can be carried out in CH$_2$Cl$_2$/HOAc^F solvent mixtures (conditions developed by Fujiwara *et al.* for the Pd/Pt-catalyzed hydroarylation)[12] without silver salts.[9] The scope of the reaction was examined, showing the possibility to engage a variety of electron-rich arenes (alkoxy, alkyl-benzenes) and alkynes (internal as well as terminal, with aryl, alkyl, keto and ester substituents). It is highly regio- and stereo-selective. Two possible reaction paths were envisioned: the *outer-sphere* route involving nucleophilic addition of the arene to the π-coordinated alkyne at gold or the *inner-sphere* route involving C–H activation of the arene followed by migratory insertion (Scheme 1).[13] No reaction intermediates could be detected at the time, but the outer-sphere mechanism was inferred indirectly from the stereochemical outcome: ANTI addition of the arene across the C≡C triple bond.
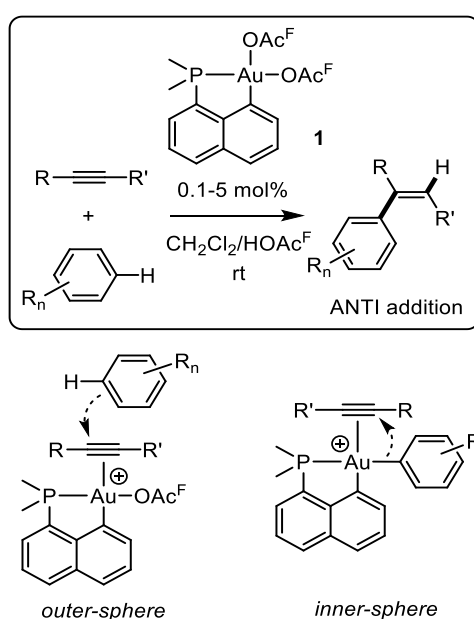

Scheme 1. Intermolecular hydroarylation of alkynes catalyzed by (P,C)-cyclometalated Au(III) complexes **1**, related key intermediates envisioned for the outer- and inner-sphere pathways.

In this work, our goal was to gain comprehensive mechanistic understanding of this transformation from experimental and computational means. We were particularly interested in authenticating the active species, resting state and key intermediates, a crucial step to improve this reaction and further develop gold(III) catalysis. To this end, the benchmark reaction between 1,3,5-trimethoxybenzene (TMB) and diphenylacetylene (DPA) was thoroughly investigated by NMR spectroscopy, mass spectrometry and DFT calculations.

Results and discussion

Experimental studies in solution

Given the propensity of gold(III) for direct metalation of arenes (as recognized by Kharash as early as in 1931 upon reaction of benzene with $AuCl_3$),[14] we considered the possibility for the (P,C)Au(OAc^F)$_2$ complex **1-iPr** to react with electron-rich arenes to give the corresponding Au(III)-aryl complexes. However, attempts for direct C−H activation of TMB at **1-iPr** proved unsuccessful; no reaction was detected after 16 hours at room temperature (Scheme 2). In contrast, the corresponding N,C-cyclometalated complex (N,C)Au(OAc^F)$_2$ (**2**), which proved inactive catalytically,[9] readily reacts with TMB to form the corresponding arylated complex **3** which was characterized by NMR spectroscopy and mass spectrometry.[15]
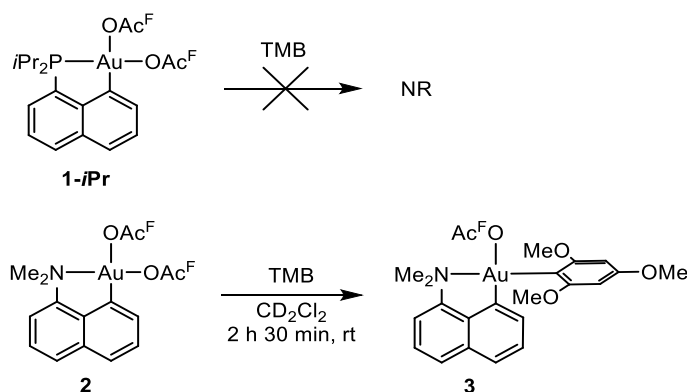

Scheme 2. (Attempted) direct metalation of 1,3,5-trimethoxybenzene (TMB) by the (P,C) Au(OAc^F)$_2$ and (N,C)Au(OAc^F)$_2$ complexes **1-iPr** and **2**.

To probe the impact of the arene C−H activation on the reaction kinetics, we then turned to deuterium labeling. The rates of two independent reactions carried out with either TMB-d_3 in CD$_2$Cl$_2$/DOAc^F or TMB in CD$_2$Cl$_2$/HOAc^F (rapid H/D exchange occurs between TMB and TFA under these conditions) were compared (Scheme 3).[15] A noticeable but relatively small kinetic isotope effect (KIE) of 1.5 was observed, which is too low for a transformation in which C−H activation of the arene at Au(III) would be the entry point and rate determining step.
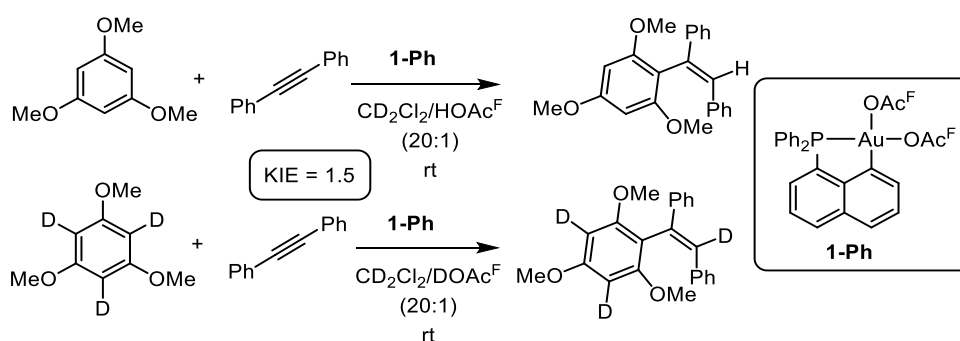

Scheme 3. Kinetic isotope effect measurement.

As mentioned previously, the (P,C)Au(OAc^F)$_2$ complexes **1** proved very active catalysts for the alkyne hydroarylation in CH$_2$Cl$_2$/HOAc^F solvent mixtures (20/1 or 1/4).[9] Trifluoroacetic acid (TFA) is presumed to activate the gold precatalyst **1** by assisting the dissociation of a trifluoroacetate anion.[3a,11] However, to facilitate the reaction monitoring and to increase the chance to characterize key intermediates, we looked for an alternative method to generate the active species. We turned to tris(pentafluorophenyl)borane (BCF) as co-catalyst, given its known ability to abstract Ac^{F}O$^-$ from Au(III) in stoichiometric reactions, as reported by Bochmann *et al.*[16] Gratifyingly, both (P,C)Au(OAc^F)$_2$ complexes **1-*i*Pr** and **1-Ph** proved catalytically active when combined with 1 equivalent of BCF. The reaction between TMB and diphenylacetylene (DPA) (1:1) was performed in pure dichloromethane at 5 mol% (Scheme 4). In both cases, 95% yield of hydroarylation product was achieved in 5 min at rt! A control reaction with BCF alone showed no conversion, demonstrating the crucial role of the gold complex.
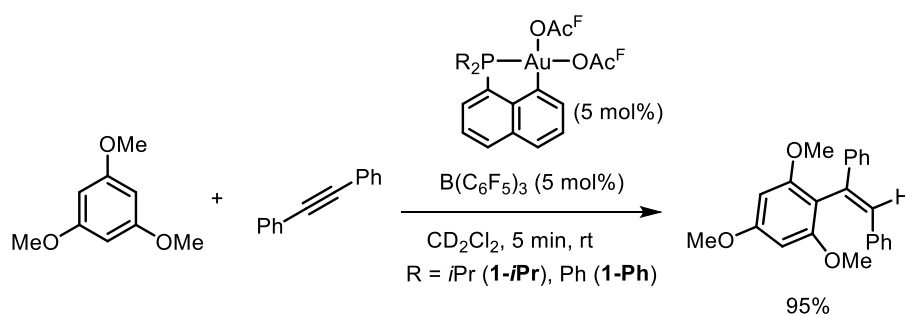

**Scheme 4.** Catalytic hydroarylation using B(C$_6$F$_5$)$_3$ (BCF) as a co-catalyst instead of HOAc^F.

To gain more insight into the nature of the active catalyst, the stoichiometric reaction of (P,C)Au(OAc^F)$_2$ complex **1-*i*Pr** and BCF in CD$_2$Cl$_2$ was investigated. Upon mixing **1-*i*Pr** and BCF at room temperature followed by immediate freezing of the sample to −80 °C, one major species was observed by multinuclear NMR analysis. It is suggested to be the ion pair [(P,C)Au(OAc^F)]$^+$[(Ac^{F}O)B(C$_6$F$_5$)$_3$]$^-$ **4-*i*Pr** where one of the OAc^F ligands has been abstracted by BCF (Scheme 5). One resonance is observed in the ^{31}P NMR spectrum at δ 138.4 (−70 °C), significantly deshielded compared to that of **1-*i*Pr** (δ 109.2, 25 °C). At −80 °C, the ^{19}F NMR spectrum shows two resonances corresponding to the two OAc^F groups at δ −74.4 and −74.7 (Figure 1), alongside with the three expected resonances from the BCF unit. The OAc^F resonance at δ −74.7 shows NOE correlations with the BCF unit, indicating that they are close in space and associated with each other (Figure 2a). Furthermore, the BCF unit shows ^{1}H-^{19}F HOE correlations with the protons of the naphthyl group indicating that we have a tight, and not separated, ion pair (Figure 2c). Warming the sample led to a broadening and eventually to the coalescence of the two ^{19}F NMR resonances (at *ca* −30 °C, Figure 1) suggesting an exchange between the OAc^F group at Au and the one at B within the NMR time scale (ΔG$^{\neq}$ estimated to *ca* 11 kcal/mol from Δv and T_c).[15] The exchange of the two OAc^F groups was further supported by a ^{19}F-^{19}F EXSY experiment performed at −60 °C (Figure 2b). In the ^{13}C NMR spectrum, two resonances corresponding to the two C=O of the OAc^F groups were observed; one at δ 159.6, in line with that observed for [(Ac^{F}O)B(C$_6$F$_5$)$_3$]$^-$ borates,[17] and one at δ 165.4, slightly deshielded compared to that of (P,C)Au(OAc^F)$_2$ **1-*i*Pr** at *ca* δ 161, in line with the higher electron-deficiency of the Au(III) center, and consistent with the 5-15 ppm deshielding found in the literature for other d/p-block elements when going from κ^1 to κ^2-coordinated OAc^F ligands.[18] These data suggest that the complex **4-*i*Pr** adopts a structure which is more towards the κ^2 than κ^1 form (see below for DFT calculations).
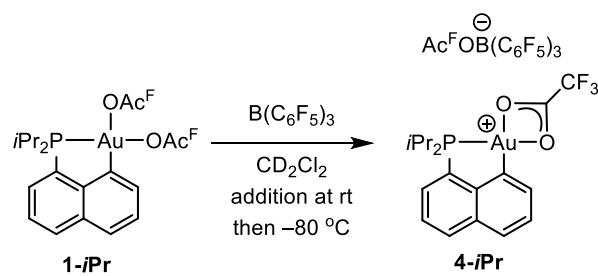
Scheme 5. Reaction of **1-*iPr*** with $B(C_6F_5)_3$.
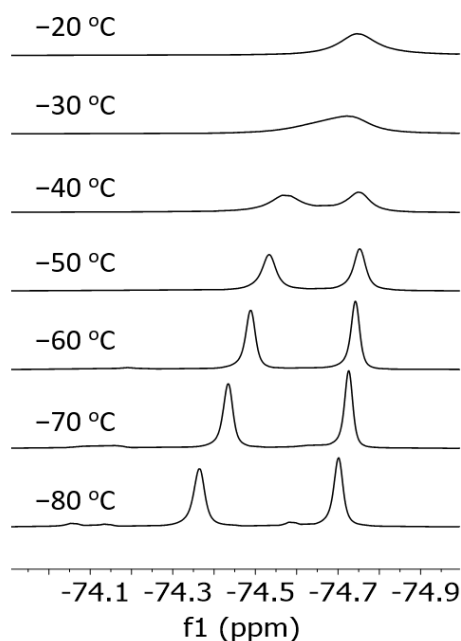
Figure 1. Stacked ^{19}F NMR (376.50 MHz, CD_2Cl_2) spectra of complex **4-*iPr*** showing the broadening and eventually the coalescence of the two OAc^F resonances with increased temperatures.
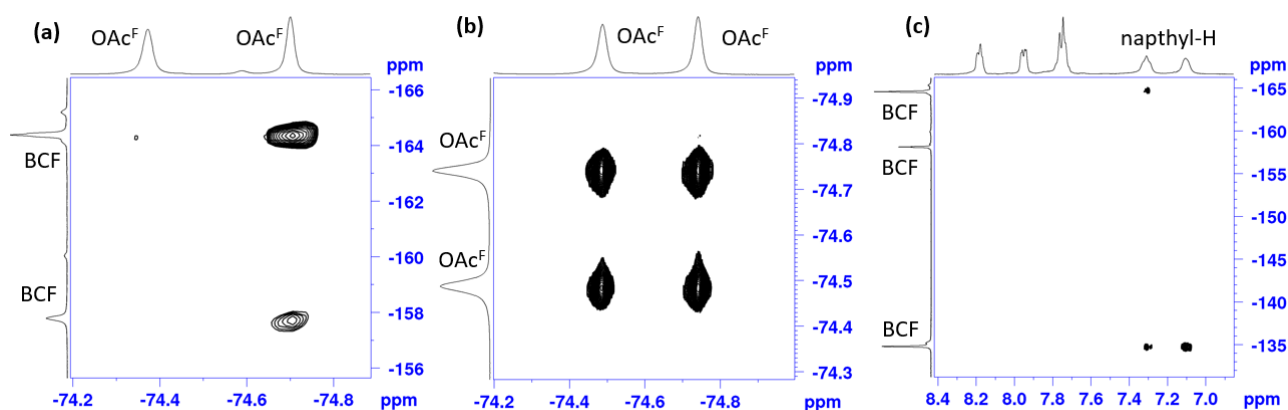
Figure 2. (a) ^{19}F-^{19}F NOESY (376.50 MHz, CD_2Cl_2, −80 °C), (b) ^{19}F-^{19}F EXSY (376.50 MHz, CD_2Cl_2, −60 °C) and (c) ^{1}H-^{19}F HOESY (400.13 MHz, CD_2Cl_2, −50 °C) spectra of complex **4-*iPr***.

To gain further insight into the formation and structure of the cationic $(iPr_2P,C)Au(OAc^F)^+$ complex, DFT calculations were carried out at the SMD(CH_2Cl_2)-B97D/SDD+f(Au),6-31G** (other atoms) level of theory. Ionization of **1-*iPr*** with BCF, affording the ion-pair $[(P,C)Au(OAc^F)]^+[(Ac^FO)B(C_6F_5)_3]^-$ is quasi thermoneutral (ΔG = −0.4 kcal/mol, Scheme S1).[15] The κ^2 form **4-*iPr*** was found as the ground-state structure (Figure 3). Two other *minima*, corresponding to the 3-coordinate T-shape κ^1 forms (complexes **4'-*iPr*** and **4''-*iPr***), were also located on the potential energy surface (PES), 3.8 and 5.7 kcal/mol higher in

energy, respectively. Low energy paths connect the κ^2 and κ^1 forms ($\Delta G^{\neq}$ 4.8 and 6.0 kcal/mol, from the κ^2 form **4-*iPr*** to the κ^1 forms **4'-*iPr*** and **4''-*iPr***, respectively). It is thus expected that the Ac^{F}O group easily slips from κ^2 to κ^1 coordination, opening a vacant coordination site at gold. The κ^2 complex **4-*iPr*** presents a distorted square planar geometry (P–Au–O$_{trans}$ 172.51°, P–Au–O$_{cis}$ 113.59° and O$_{cis}$–Au–O$_{trans}$ 58.92°) with two quasi-similar Au–O bonds (2.242 and 2.288 Å for O *trans* to P and C, respectively). This quasi-symmetric structure makes complex **4-*iPr*** somewhat reminiscent of the (P,C)Au(π-allyl)$^+$ species we recently reported.[19] Calculations were also carried out on the related Ph-substituted complex (Ph$_2$P,C)Au(OAc^F)$^+$ (Figure S27).[15] The picture is very similar: the κ^2 form is the ground state, the respective κ^1 forms are found 3.7-4.0 kcal/mol higher in energy.
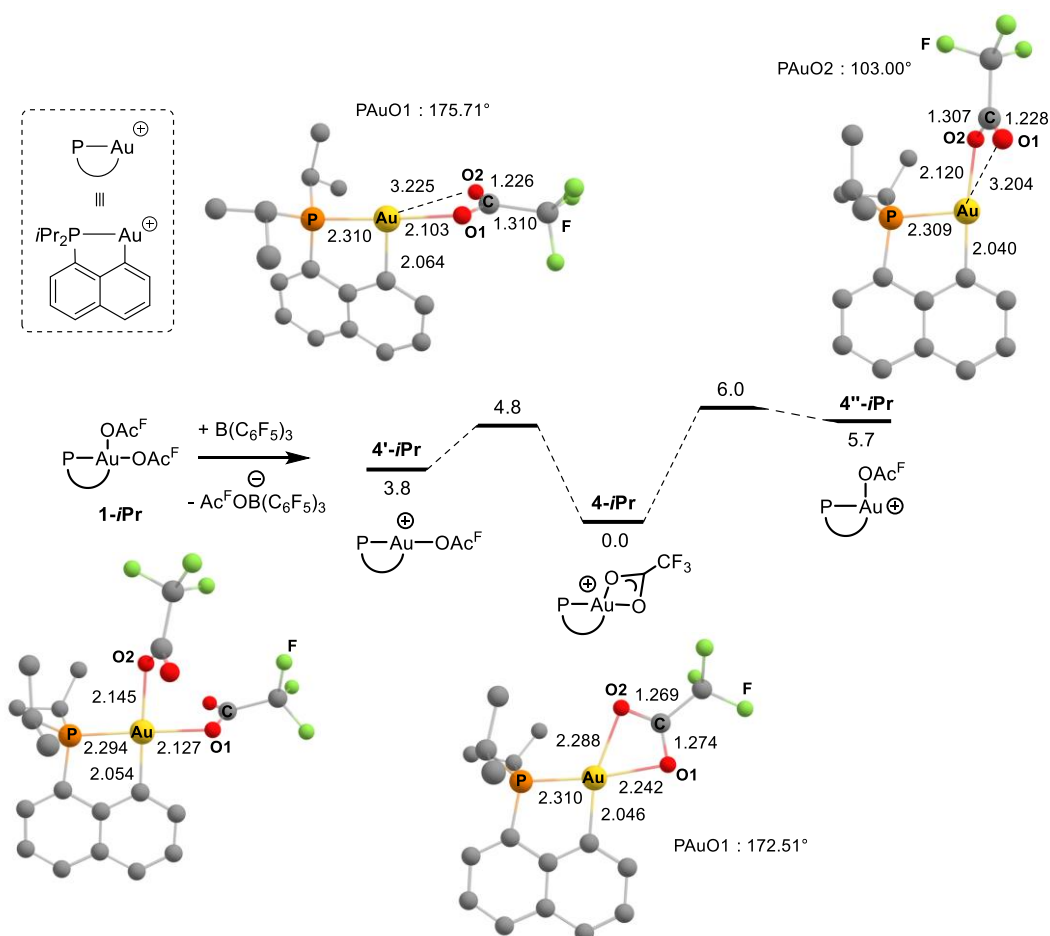
Figure 3. Ionization of the (*iPr*$_2$P,C)Au(OAc^F)$_2$ complex **1-*iPr*** with BCF, structures and interconversion of the κ^2 and κ^1 forms of the ensuing (*iPr*$_2$P,C)Au(OAc^F)$^+$ complex **4-*iPr***, computed at the SMD(CH$_2$Cl$_2$)-B97D/SDD+f(Au), 6-31G** (other atoms) level of theory. Bond lengths and bond angles are given in Å and °, respectively. Relative stability (ΔG) in kcal/mol.

The only precedent of a cationic cyclometalated carboxylate Au(III) complex we are aware of is the (N,C)Au(OAc^F)$^+$ complex (N,C = 2-(*p*-tolyl)pyridine) proposed by Nova, Tilset *et al.* to account for the addition of O-nucleophiles to alkenes and alkynes.[3a,11a] Comparing the two systems reveals pronounced differences. The two κ^1 forms of the N,C-cyclometalated complex significantly differs in energy: the one with the vacant coordination site *trans* to the stronger σ-donating C atom is 14.3 kcal/mol more stable than the one with the vacant coordination site *trans* to the N atom (calculations performed at PBE0-D3 level) and it is actually the ground-state, 0.9 kcal/mol more stable than the κ^2 form. The κ^2 form adopts a much more dissymmetric structure than our (P,C) system, with Au–O bond lengths of 2.08 and 2.39 Å, in line with the larger difference in *trans* influence between N and C in the tolylpridine system compared to P and C in the (P,C)-cyclometalated system.[11a]

The $[(P,C)Au(OAc^F)]^+[(Ac^FO)B(C_6F_5)_3]^-$ complex **4-iPr** reacts readily with 1 equivalent of TMB at −80 °C. Multinuclear NMR characterization at −40 °C shows the formation of the corresponding C-adduct **5-iPr** (Scheme 6). No sign of C−H auration was observed, even over time or with increased temperature. The complex is stable up to *ca* −20°C, but decomposes upon warming to room temperature. The connectivity between TMB and the gold complex was confirmed by a ^1H-^{31}P HMBC experiment where a correlation between the *ipso* hydrogen atom (H_{ipso}) of the TMB unit and P (δ 106.0) was observed (Figure 4a). Several features diagnostic of the η^1-coordination of C_{ipso} were observed by NMR: (*i*) the shielding of the respective CH_{ipso} ^1H and ^{13}C NMR resonances (δ 5.52 and δ 51.4, respectively), (*ii*) the decrease of the associated $^1J_{CH}$ coupling constant (150 Hz, *vs* 168 Hz for CH_{meta}) in line with some change in hybridization (from sp^2 towards sp^3, Figure 4b) and (*iii*) the deshielding of the ^{13}C NMR C(OMe) resonances (from δ 164.4 in free TMB to δ 180.6 and 183.0 for the *ortho* and *para* resonances, respectively), in very good agreement with that predicted computationally (Table S2).[15] Furthermore, a ^1H-^1H NOE correlation between H_{ipso} and the *i*Pr ^1H NMR resonances (Figure 4c) suggests the formation of the isomer with the TMB moiety *cis* to P, which is actually found by DFT calculations to be the most stable (see below).[20]
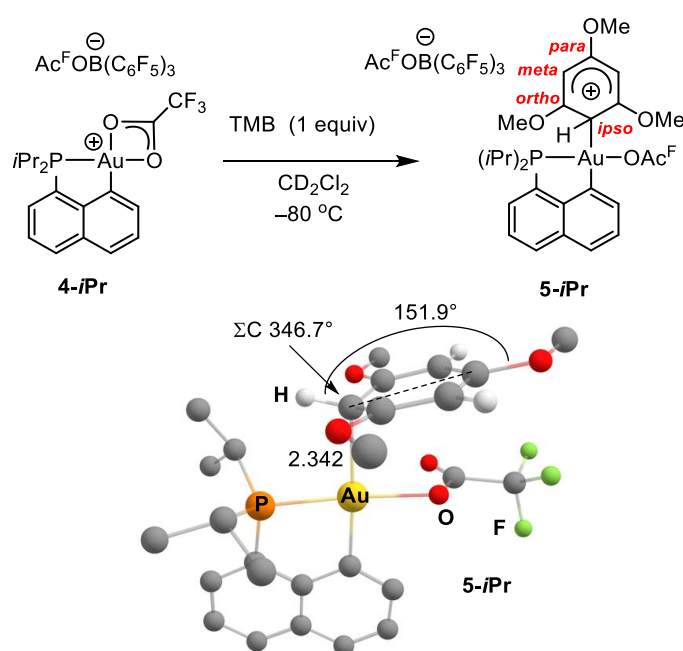
Scheme 6. Formation and optimized structure of the η^1 C-adduct **5-iPr** (a Wheland-type complex) upon reaction of **4-iPr** with TMB (distances in Å and angles in °).
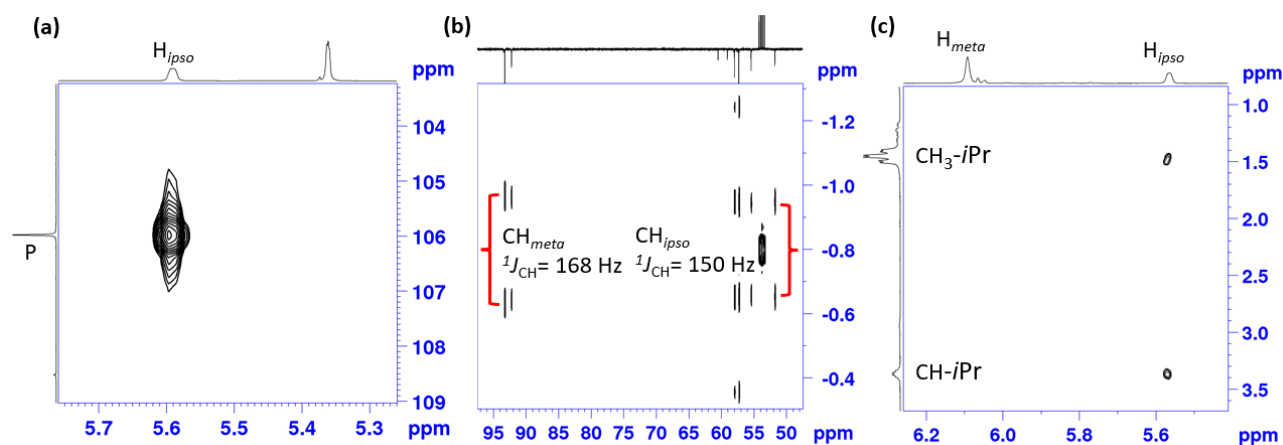
**Figure 4.** (a) ^1H-^{31}P HMBC (500.11 MHz, CD_2Cl_2, −30 °C), (b) *J*-resolved ^{13}C NMR (125.75 MHz, CD_2Cl_2, −23 °C), and (c) ^1H-^1H NOESY (400.13 MHz, CD_2Cl_2, −30 °C) spectra of complex **5-iPr**.

8

The coordination of TMB to complex **4-*iPr*** was investigated computationally (Figures S28-S29 and Table S2).[15] Four *minima* were found on the PES, corresponding to C and O-adducts, with OAc^F *trans* or *cis* to P. The ground state is the C-adduct with the OAc^F group *trans* to P, in agreement with that observed experimentally. The O-adducts are found ≥8.8 kcal/mol higher in energy and the C-adduct with OAc^F *cis* to P is found 6.6 kcal/mol higher in energy. The structure optimized by DFT (Scheme 6) corresponds to a σ rather than π-complex of the arene. It displays a short C_{ipso}–Au distance (2.342 Å), long C_{ortho}–Au distances (3.002 and 3.014 Å) and the C_{ipso} carbon is noticeably pyramidalized (as apparent for the sum of bond angles ΣC 346.7° and the H−C_{ipso}···C_{para}−O dihedral angle of 151.9°). These geometrical features are indicative of η^1-coordination of TMB, in line with that observed experimentally. The η^1 C-coordinated complex **5-*iPr*** is a Wheland-type structure representing an advanced stage in the C−H auration process at gold. To the best of our knowledge, such a coordination mode was until now unprecedented experimentally for gold.[21] In a computational study by Tilset, Swang and co-workers in 2010, the Wheland complex [(N,N)AuPh(η^1-C_6H_6)]$^{2+}$ (N,N = 2,2'-bipyridine) was found as the energy *minimum* of the reaction of [(N,N)AuPh]$^{2+}$ with benzene, but attempts at gaining experimental evidence for this complex failed.[22] In fact, only a few Au(III) arene complexes have been reported so far.[23] In these complexes, a pendant arene is π coordinated to gold in an η^1 or η^2 fashion. Of note, a few geminally diaurated Au(I) aryl complexes [(LAu)$_2$(μ-aryl)]$^+$ have also been authenticated, these can be regarded as analogues to Wheland complexes due to the LAu$^+$ fragment being isolobal to H$^+$.[24]

The reactivity of **4-*iPr*** towards DPA was also investigated, but in this case no significant reactivity was observed and the π-complex **6-*iPr*** could not be identified by NMR spectroscopy (Scheme 7).[16a,25]
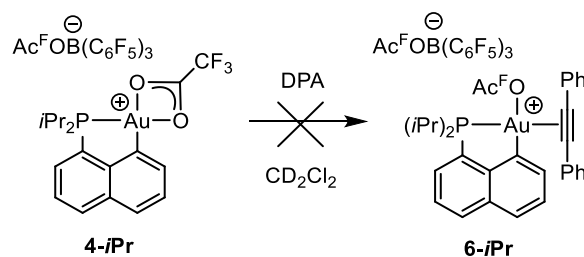
Scheme 7. Attempted formation of the π-alkyne complex **6-*iPr*** upon reaction of **4-*iPr*** with DPA in CD$_2$Cl$_2$ solution.

Following the finding that complex **4-*iPr*** readily reacts with TMB forming the η^1 C-adduct **5-*iPr*,** we were interested in studying the reactivity of **5-*iPr*** towards DPA. Complex **5-*iPr*** was generated *in situ* at −80 °C in CD$_2$Cl$_2$ and treated with DPA. A reaction ensued at −40 °C, leading to the formation of the same hydroarylation product as was obtained under the catalytic conditions.[26] This suggests that the formation of complex **5-*iPr*** is reversible and that it acts as an off-cycle resting state during the catalysis. Following this, we were interested to see if upon lowering the temperature of the catalytic reaction, we would be able to detect **5-*iPr*** during the catalysis. And indeed, upon performing the catalytic reaction at −35 °C, we were able to authenticate complex **5-*iPr*** by ^{31}P NMR and ^{1}H NMR.[15]

Experimental studies in the gas phase
    The cationic nature of the involved Au(III) species makes mass spectrometry (MS) well-adapted to study such a transformation and to try to catch elusive intermediates. Tandem mass spectrometry coupled with electrospray ionization (ESI) has proven to be a valuable tool for elucidating various organometallic structures and for studying their reactivity in the gas phase.[27] To draw a parallel with the studies performed in solution, the same substrates, *i.e.* DPA and TMB, were to be used. However, these compounds are not volatile enough to be introduced into standard collision cells under the simple action of the vacuum that resides in the spectrometer. A device consisting of a heated introduction line into the

first collision cell of our instrument was therefore built (Figure S24).[15] With such a device, less volatile reagents could be introduced into the first collision cell in sufficient quantities to form ion-molecule adducts. The next step was to find source conditions to generate the cationic complex $(i\text{Pr}_2\text{P,C})\text{Au}(\text{OAc}^F)^+$ **4-iPr** by dissociating a trifluoroacetate from the initial complex $(i\text{Pr}_2\text{P,C})\text{Au}(\text{OAc}^F)_2$ **1-iPr**. This could be achieved by infusing the neutral complex in acetonitrile with a cone voltage at 50 V. The signal at m/z 553 corresponding to **4-iPr** is shown in Figure 5. The theoretical isotopic profile is superimposed in red on the experimental peaks and shows a perfect agreement.
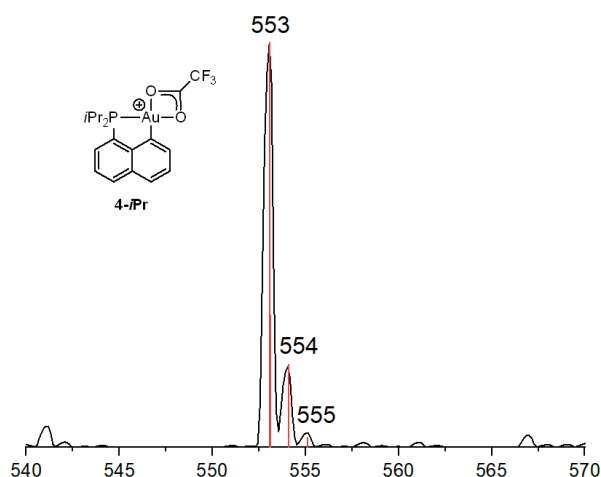
Figure 5. MS spectrum of $[(i\text{Pr}_2\text{P,C})\text{Au}(\text{OAc}^F)_2]$ **1-iPr** (5.10^{-5} M in CH_3CN), theoretical isotopic profile for the cationic complex $(i\text{Pr}_2\text{P,C})\text{Au}(\text{OAc}^F)^+$ **4-iPr** in red.

Once the cationic complex $(i\text{Pr}_2\text{P,C})\text{Au}(\text{OAc}^F)^+$ **4-iPr** was generated in the source of the mass spectrometer, we sought to observe the formation of adducts with each of the organic substrates. With the help of the heated line, we were able to observe each of the expected adducts whose collision-induced dissociation (CID) spectra are presented in Figure 6. These spectra were obtained by first performing an ion-molecule reaction between the cation **4-iPr** (m/z 553) and DPA (left side, heated line 140°C), then by selecting the adduct ion at m/z 731 by the first quadrupole and by colliding it with nitrogen ($P(N_2) = 1.10^{-3}$ mbar, $E_{COM} = 0.41$ eV) in the second collision cell. The same procedure was followed with TMB (right side, heated line 120°C) to generate and dissociate the respective adduct cation at m/z 721.
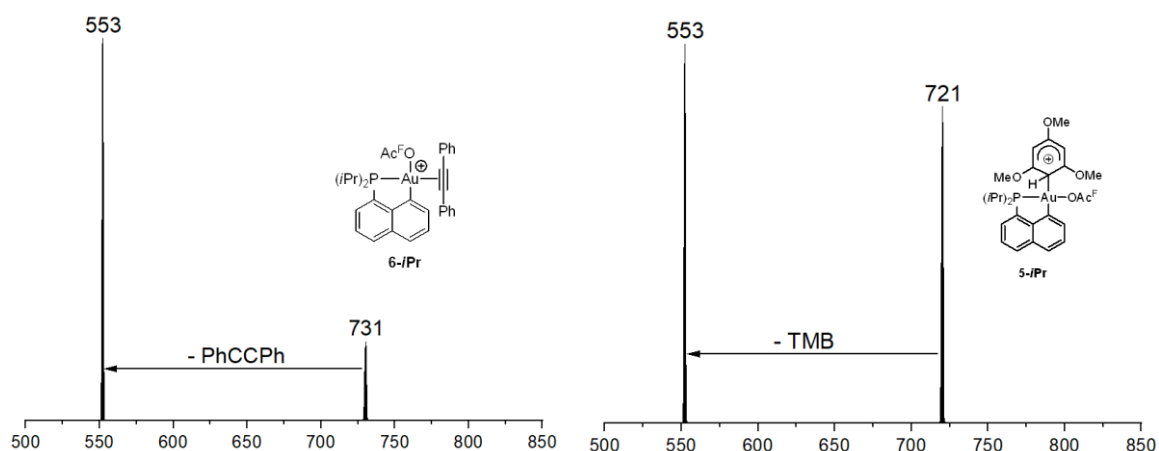

Figure 6. CID spectra of the adduct ions m/z 731 (DPA) and m/z 721 (TMB), with N_2 as collision gas.

While it was not possible to characterize a coordination complex between **4-iPr** and DPA in solution, it proved possible in the gas phase. This adduct **6-iPr** seems however relatively fragile judging

by the low collision energy required to fragment it. Comparatively, the cation molecule adduct with TMB **5-*iPr*** forms very well and seems stronger than the one with DPA, as qualitatively supported by the ratio of intensities of the adduct and fragment signals in the CID spectra: 0.22 for DPA (m/z 721/553) *versus* 0.93 for TMB (m/z 731/553).

With these encouraging results, we then attempted to form a ternary adduct by introducing the two reactants together *via* the heated line (in the same flask at 140°C). To our great satisfaction, we were able to produce an ion at m/z 899 (Figure 7a), the expected m/z for such a complex. Here also, the theoretical isotopic profile (in red) matched well with that observed experimentally.
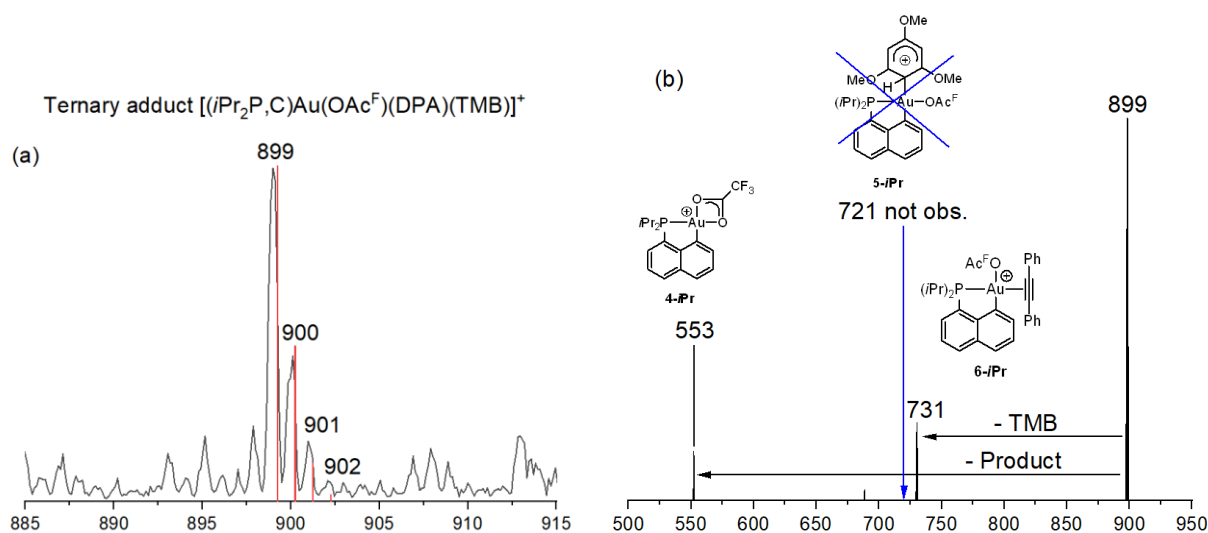
Figure 7. (a) MS spectrum obtained during ion-molecule reaction of (*iPr₂P,C*)Au(OAc^F)$^+$ **4-*iPr*** (generated from [(*iPr₂P,C*)Au(OAc^F)₂] **1-*iPr*** at 5.10^{-5} M in CH₃CN) with DPA and TMB (140°C), theoretical isotopic profile in red. (b) CID spectrum of the m/z 899 ternary adduct ion, with N₂ as collision gas (E$_{COM}$ = 0.30 eV).

Produced with sufficient abundance, we were able to break the m/z 899 ion by CID with dinitrogen (Figure 7b) and the fragments obtained proved to be very instructive. Indeed, upon fragmentation, the ternary adduct gives a small amount of the m/z 731 cation **6-*iPr*** which corresponds to the loss of TMB but does not give the m/z 721 cation **5-*iPr*** corresponding to the loss of DPA. The major fragment ion corresponds to the "naked" cationic complex **4-*iPr*** at m/z 553. This suggests that the alkyne, once coordinated to gold, forms a bond with TMB and that the coupling product of the alkyne and arene is then lost to give the native cationic complex **4-*iPr***. This observation supports the outer-sphere mechanism as opposed to the inner-sphere path.

DFT study of the reaction profiles

In parallel with the experimental studies, the energy profiles for the hydroarylation reaction between TMB and DPA were computed starting from the cationic complex (*iPr₂P,C*)Au(OAc^F)$^+$ **4-*iPr*** as the active species. Both the outer- and inner-sphere paths were examined. Special attention was devoted to the C–C bond formation process which is the stereo-defining step (*trans* addition). Protodeauration then occurs with retention of configuration. Note that the incoming substrate may bind to gold *cis* or *trans* to P. Both scenarios were considered, but little differences were found, in line with the small electronic dissymmetry of the P,C ligand (the positions *trans* to P and C are about equivalent electronically). This contrasts with the high electronic dissymmetry of N,C-ligated Au(III) complexes, as previously noticed.[3a,11a,28]

Outer-sphere path of C–C bond formation

The outer-sphere mechanism was studied first (Figure 8). This pathway involves π-coordination of DPA to gold. It is downhill in energy from the κ²-(*i*Pr₂P,C)Au(OAc^F)⁺ complex **4-*i*Pr**, by ΔG −9.7 kcal/mol for the coordination of DPA *trans* to P (by −5.4 kcal/mol *cis* to P). σ-Coordination of TMB to give the Wheland-type complex **5-*i*Pr** is further downhill in energy (at −16.1 kcal/mol for the coordination *trans* to C). Nucleophilic addition of the arene to the π-activated alkyne proceeds very easily. The activation barrier for the addition of TMB to DPA is of only 2.6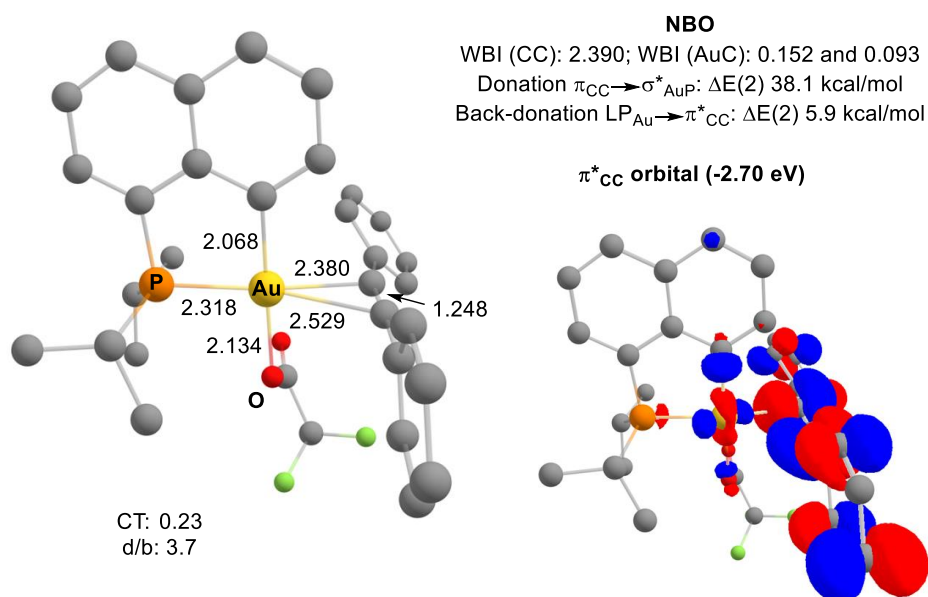–3.4 kcal/mol and the reaction is downhill in energy by 10.9–15.2 kcal/mol. It results in vinyl Au(III) complexes with the aryl group *trans* to gold (in line with the formation of the experimentally obtained ANTI addition product after stereoretentive protodeauration). Of note, the entry point (and likely rate-determining step) of the outer-sphere mechanism is the displacement of TMB by DPA at Au(III) (pre-equilibrium).[29]
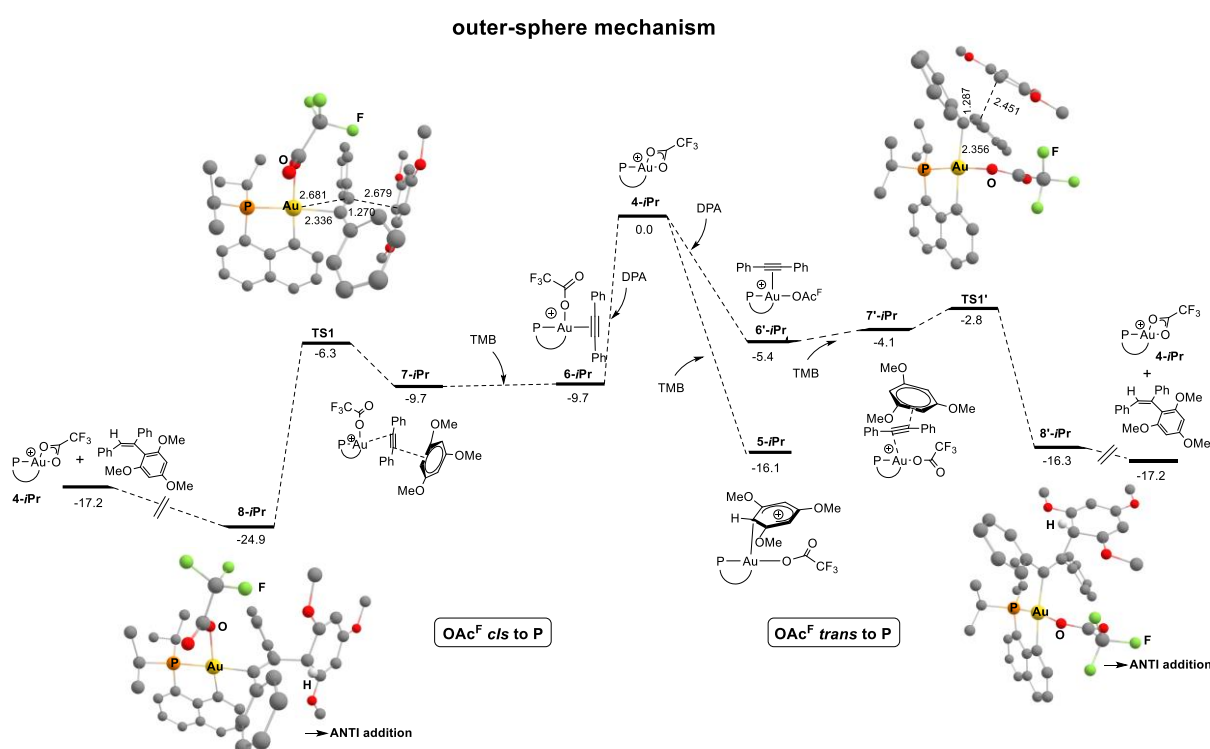
Figure 8. Energy profile for the outer-sphere mechanism from complex **4-*i*Pr** (ΔG values in kcal/mol) computed at the SMD(CH₂Cl₂)-B97D/SDD+f(Au)/6-31G**(other atoms) level of theory taking into account dichloromethane effects with the SMD model.

In this path, the key intermediates are the π-alkyne Au(III) complexes **6/6'-*i*Pr**. In contrast with the TMB adduct, the most stable isomer is the one with DPA coordinated *trans* to P, **6-*i*Pr**. The structure of **6/6'-*i*Pr** was analyzed in-depth (Figure 9). In line with the geometrical features of previously reported π-alkyne Au(III) complexes,[16a,21,25] the C≡C triple bond is oriented perpendicularly to the Au coordination plane (CCAuP torsion angles of -86.2° and 96.2° for the coordination of DPA *cis* and *trans* to P, respectively, Figure S29).[15] It is only slightly elongated and marginally deviates from linearity (DPA *cis* to P: C≡C 1.243 Å, C≡C−C(Ph) 168.79°; DPA *trans* to P: C≡C 1.248 Å, C≡C−C(Ph) 163.54°; free PhCCPh: C≡C 1.228 Å, C≡C−C(Ph) 180.0°). Charge-Decomposition Analyses (CDA) and Natural Bond Orbital (NBO) analyses reveal that π$_{C=C}$ → Au donation largely prevails over Au → π*$_{C=C}$ back-donation: d/b ratio higher than 3.5; ΔE(2) ~ 30–40 and 5–6 kcal/mol, respectively (Tables S3-S4). Consistently, the alkyne coordination to gold is associated with a substantial electron transfer by about 0.21–0.23 e, in line with the electrophilic activation of the C≡C triple bond. The associated π*$_{CC}$ orbitals, found as LUMO+1, are

low in energy (−2.70 to −2.78 eV). Similar geometrical and electronic features were obtained for the adducts of DPA to the Ph-substituted complex (Ph$_2$P,C)Au(OAc^F)$^+$ **4-Ph** (Figure S30).[15]

NBO
WBI (CC): 2.390; WBI (AuC): 0.152 and 0.093
Donation $\pi_{CC} \rightarrow \sigma^*_{AuP}$: $\Delta E(2)$ 38.1 kcal/mol
Back-donation $LP_{Au} \rightarrow \pi^*_{CC}$: $\Delta E(2)$ 5.9 kcal/mol

π^*_{CC} **orbital (-2.70 eV)**

CT: 0.23
d/b: 3.7

Figure 9. Optimized geometry of the key (*i*Pr$_2$P,C)Au(OAc^F)(π-DPA)$^+$ complex **6-*iPr*** (distances in Å), selected CDA and NBO data pertaining to the bonding situation (donation/back-donation ratio d/b, charge transfer from DPA to gold CT, Wiberg Bond indexes WBI and stabilizing interactions $\Delta E(2)$ in kcal/mol for DPA→Au donation and Au→DPA back-donation). Plot of the vacant orbital mainly localized on $\pi^*_{C=C}$ orbital (LUMO+1) with cutoff: 0.04.

Inner-sphere path of C–C bond formation

For sake of comprehensiveness, the inner-sphere path was also studied for both isomers with the OAc^F group *trans* or *cis* to P (Figures 10 and S31).[15] The computed energy profiles are quite similar. Consequently, only the most favorable one, with OAc^F *trans* to P, will be discussed here. Upon reaction of TMB with the cationic complex (*i*Pr$_2$P,C)Au(OAc^F)$^+$ **4-*iPr***, C coordination is favored over O coordination by about 8.8 kcal/mol. The Wheland complex described above is downhill in energy by 16.1 kcal/mol, making the coordination of TMB stronger than that of DPA (ΔG −9.7 kcal/mol in the latter case, Figure S29).[15] The resulting σ-complex is the resting state of the process. Auration of the arene *via* a Concerted Metalation-Deprotonation (CMD)-type path, with rotation around the Au–C$_{ipso}$ bond and proton transfer from TMB to the OAc^F ligand occurs with a rather large activation barrier of 17.3 kcal/mol. Then, the exchange of Ac^{F}OH for DPA at gold is about thermoneutral (ΔG 1.6 kcal/mol). Finally, migratory insertion of the alkyne into the Au–aryl bond proceeds with an activation barrier of 8.6 kcal/mol, resulting in *cis*-addition of Ar–H across the C≡C bond. Overall, the barrier for the C–C bond formation (from the Wheland-type complex **5-*iPr*** to the migratory insertion transition state) reaches 26.9 kcal/mol (28.1 kcal/mol for the isomer with OAc^F *cis* to P). These barriers are significantly higher than those computed for the outer-sphere mechanism, meaning that the inner-sphere path is not competitive.

Figure 10. Energy profile for the inner-sphere mechanism from complex **4-iPr** with coordination of TMB *cis* to P (ΔG values in kcal/mol) computed at the SMD(CH₂Cl₂)-B97D/SDD+f(Au)/6-31G**(other atoms) level of theory taking into account dichloromethane effects with the SMD model.

Protodeauration

As previously pointed out for other gold-catalyzed transformations, the protodeauration step should not be neglected and may be rate-determining, especially when the preceding C–C/C–X bond formation processes involve very low activation barriers.[30] However, under our catalytic conditions (CH₂Cl₂/HOAc^F solvent mixture), protodeauration is expected to be quite facile and not to compensate for the high difference in activation barriers between the outer- and inner-sphere paths.[31] Previous computational studies have shown that the protodeauration step may be rather complex;[3a,30,32] it is actually quite challenging to account for comprehensively and reliably. In our case, many paths are conceivable, involving or not assistance by the OAc^F moiety at gold. One or several external TFA or TMB molecules may also participate and act as proton shuttles.[32a,33] To support the easiness of the protodeauration, we reasoned that a simple path would involve TFA adducts of the Au(III) vinyl complexes resulting from the arene/alkyne coupling at gold. We considered the Au(III) vinyl complexes resulting from both the outer- and inner-sphere mechanisms and compared them (Scheme 8). The tautomeric form **13-iPr** of **8-iPr**, in which the proton at C_ipso (TMB) is transferred to the OAc^F group at gold is only slightly higher in energy (ΔG 4.8 kcal/mol), and protolytic cleavage of the Au(III)–vinyl bond is then facile, with an activation barrier of only 2.0 kcal/mol (Figure S33).[15] As for the migratory-insertion complex **12-iPr**, coordination of TFA to Au(III) is downhill in energy by 8.6 kcal/mol and protodeauration then proceeds readily (ΔG‡ 3.8 kcal/mol) (Figure S34). Although these two protodeauration paths may not be the most favorable ones, these calculations indicate that this step is in both cases easy and it is unlikely

to make a noticeable difference between the outer- and inner-sphere mechanisms, in contrast to the C–C bond formation step.

outer-sphere mechanism

inner-sphere mechanism

Scheme 8. Protodeauration processes computed from Au(III) vinyl complexes resulting from outer- and inner-sphere C–C bond formation.

Conclusion

Thanks to the combined use of NMR spectroscopy, mass spectrometry and DFT calculations, we have gained detailed mechanistic insights into the hydroarylation of alkynes catalyzed by (P,C)-cyclometalated Au(III) complexes. Several key intermediates have been authenticated experimentally and the energy profiles for the outer- and inner-sphere paths have been thoroughly compared computationally. The characterized intermediates turned to be original Au(III) complexes. A cationic Au(III) complex **4-*iPr*** with a κ^2-coordinated carboxylate was spectroscopically observed for the first time. It easily releases a coordination site at gold(III) upon κ^2 to κ^1 slippage and stands as the active species. Addition of TMB to **4-*iPr*** results in an unprecedented σ-arene complex **5-*iPr***. This Wheland-type Au(III) complex represents an advanced stage in the C–H auration of arenes. Coordination of DPA to the cationic Au(III) complex **4-*iPr*** has also been evidenced by mass spectrometry. The ensuing π-complex **6-*iPr*** plays a pivotal role, it readily undergoes outer-sphere nucleophilic addition of the arene, as supported by CID experiments and DFT calculations.

Besides advancing our understanding of the Au(III)-catalyzed alkyne hydroarylation, these results provide valuable information about the way Au(III) complexes bind and activate alkynes and arenes, substrates of broad synthetic interest. The cyclometalated ligand brings stability to the Au(III) species all over the catalytic cycle and offers a handle to tune and optimize the system. To this end, future work will aim to vary the steric and electronic properties of the ligand, and to study the influence on the formation, stability and reactivity of the different key intermediates.

Acknowledgements

Supporting Information

The Supporting Information is available free of charge at htttps//pubs.acs.org/doi/.
   Experimental and computational details, analytical data and NMR spectra (PDF)
   Optimized cartesian coordinates (XYZ)

References and Notes

(1) (a) Schmidbaur, H.; Schier, A. Gold(III) Compounds for Homogeneous Catalysis: Preparation, Reaction Conditions, and Scope of Application. *Arab. J. Sci. Eng.* **2012**, *37* (5), 1187-1225. DOI: 10.1007/s13369-012-0313-3; (b) Rocchigiani, L.; Bochmann, M. Recent Advances in Gold(III) Chemistry: Structure, Bonding, Reactivity, and Role in Homogeneous Catalysis. *Chem. Rev.* **2021**, *121* (14), 8364-8451. DOI: 10.1021/acs.chemrev.0c00552

(2) (a) Wu, C.-Y.; Horibe, T.; Jacobsen, C. B.; Toste, F. D. Stable gold(III) catalysts by oxidative addition of a carbon–carbon bond. *Nature* **2015**, *517*, 449-454. DOI: 10.1038/nature14104; (b) Chintawar, C. C.; Yadav, A. K.; Kumar, A.; Sancheti, S. P.; Patil, N. T. Divergent Gold Catalysis: Unlocking Molecular Diversity through Catalyst Control. *Chem. Rev.* **2021**, *121* (14), 8478-8558. DOI: 10.1021/acs.chemrev.0c00903

(3) (a) Holmsen, M. S. M.; Nova, A.; Balcells, D.; Langseth, E.; Øien-Ødegaard, S.; Heyn, R. H.; Tilset, M.; Laurenczy, G. *trans*-Mutation at Gold(III): A Mechanistic Study of a Catalytic Acetylene Functionalization *via* a Double Insertion Pathway. *ACS Catal.* **2017**, *7* (8), 5023-5034. DOI: 10.1021/acscatal.7b01364; (b) Holmsen, M. S. M.; Nova, A.; Hylland, K.; Wragg, D. S.; Øien-Ødegaard, S.; Heyn, R. H.; Tilset, M. Synthesis of a (N,C,C) Au(III) pincer complex via C$_{sp3}$–H bond activation: increasing catalyst robustness by rational catalyst design. *Chem. Commun.* **2018**, *54* (79), 11104-11107. DOI: 10.1039/C8CC05489D

(4) Reiersølmoen, A. C.; Csókás, D.; Pápai, I.; Fiksdahl, A.; Erdélyi, M. Mechanism of Au(III)-Mediated Alkoxycyclization of a 1,6-Enyne. *J. Am. Chem. Soc.* **2019**, *141* (45), 18221-18229. DOI: 10.1021/jacs.9b09108

(5) Reiersølmoen, A. C.; Csókás, D.; Øien-Ødegaard, S.; Vanderkooy, A.; Gupta, A. K.; Carlsson, A.-C. C.; Orthaber, A.; Fiksdahl, A.; Pápai, I.; Erdélyi, M. Catalytic Activity of *trans*-Bis(pyridine)gold Complexes. *J. Am. Chem. Soc.* **2020**, *142* (13), 6439-6446. DOI: 10.1021/jacs.0c01941

(6) Kumar, R.; Nevado, C. Cyclometalated Gold(III) Complexes: Synthesis, Reactivity, and Physicochemical Properties. *Angew. Chem. Int. Ed.* **2017**, *56* (8), 1994-2015. DOI: 10.1002/anie.201607225

(7) For selected examples, see: (a) Joost, M.; Zeineddine, A.; Estévez, L.; Mallet–Ladeira, S.; Miqueu, K.; Amgoune, A.; Bourissou, D. Facile Oxidative Addition of Aryl Iodides to Gold(I) by Ligand Design: Bending Turns on Reactivity. *J. Am. Chem. Soc.* **2014**, *136* (42), 14654-14657. DOI: 10.1021/ja506978c; (b) Rekhroukh, F.; Estévez, L.; Bijani, C.; Miqueu, K.; Amgoune, A.; Bourissou, D. Experimental and Theoretical Evidence for an Agostic Interaction in a Gold(III) Complex. *Angew. Chem. Int. Ed.* **2016**, *55* (10), 3414-3418. DOI: 10.1002/anie.201511111; (c) Rekhroukh, F.; Estevez, L.; Mallet-Ladeira, S.; Miqueu, K.; Amgoune, A.; Bourissou, D. β-Hydride Elimination at Low-Coordinate Gold(III) Centers. *J. Am. Chem. Soc.* **2016**, *138* (36), 11920-11929. DOI: 10.1021/jacs.6b07035; (d) Pujol, A.; Lafage, M.; Rekhroukh, F.; Saffon-

Merceron, N.; Amgoune, A.; Bourissou, D.; Nebra, N.; Fustier-Boutignon, M.; Mézailles, N. A Nucleophilic Gold(III) Carbene Complex. *Angew. Chem. Int. Ed.* **2017**, *56* (40), 12264-12267. DOI: 10.1002/anie.201706197; (e) Zeineddine, A.; Estévez, L.; Mallet-Ladeira, S.; Miqueu, K.; Amgoune, A.; Bourissou, D. Rational development of catalytic Au(I)/Au(III) arylation involving mild oxidative addition of aryl halides. *Nat. Commun.* **2017**, *8* (1), 565. DOI: 10.1038/s41467-017-00672-8; (f) Rigoulet, M.; Thillaye du Boullay, O.; Amgoune, A.; Bourissou, D. Gold(I)/Gold(III) Catalysis that Merges Oxidative Addition and π-Alkene Activation. *Angew. Chem. Int. Ed.* **2020**, *59* (38), 16625-16630. DOI: 10.1002/anie.202006074; (g) Szalóki, G.; Babinot, J.; Martin-Diaconescu, V.; Mallet-Ladeira, S.; García-Rodeja, Y.; Miqueu, K.; Bourissou, D. Ligand-enabled oxidation of gold(I) complexes with o-quinones. *Chem. Sci.* **2022**, *13* (35), 10499-10505. DOI: 10.1039/D2SC03724F

(8) Guenther, J.; Mallet-Ladeira, S.; Estevez, L.; Miqueu, K.; Amgoune, A.; Bourissou, D. Activation of Aryl Halides at Gold(I): Practical Synthesis of (P,C) Cyclometalated Gold(III) Complexes. *J. Am. Chem. Soc.* **2014**, *136* (5), 1778-1781. DOI: 10.1021/ja412432k

(9) Blons, C.; Mallet-Ladeira, S.; Amgoune, A.; Bourissou, D. (P,C) Cyclometalated Gold(III) Complexes: Highly Active Catalysts for the Hydroarylation of Alkynes. *Angew. Chem. Int. Ed.* **2018**, *57* (36), 11732-11736. DOI: 10.1002/anie.201807106

(10) For a recent review on gold-catalyzed hydroarylation of alkynes, see: Ghosh, T.; Chatterjee, J.; Bhakta, S. Gold-catalyzed hydroarylation reactions: a comprehensive overview. *Org. Biomol. Chem.* **2022**, *20* (36), 7151-7187. DOI: 10.1039/D2OB00960A

(11) (a) Langseth, E.; Nova, A.; Tråseth, E. A.; Rise, F.; Øien, S.; Heyn, R. H.; Tilset, M. A Gold Exchange: A Mechanistic Study of a Reversible, Formal Ethylene Insertion into a Gold(III)–Oxygen Bond. *J. Am. Chem. Soc.* **2014**, *136* (28), 10104-10115. DOI: 10.1021/ja504554u; (b) Hylland, K. T.; Schmidtke, I. L.; Wragg, D. S.; Nova, A.; Tilset, M. Synthesis of substituted (N,C) and (N,C,C) Au(III) complexes: the influence of sterics and electronics on cyclometalation reactions. *Dalton Trans.* **2022**, *51* (13), 5082-5097. DOI: 10.1039/D2DT00371F

(12) (a) Jia, C.; Piao, D.; Oyamada, J.; Lu, W.; Kitamura, T.; Fujiwara, Y. Efficient Activation of Aromatic C-H Bonds for Addition to C-C Multiple Bonds. *Science* **2000**, *287* (5460), 1992-1995. DOI: 10.1126/science.287.5460.1992; (b) Jia, C.; Lu, W.; Oyamada, J.; Kitamura, T.; Matsuda, K.; Irie, M.; Fujiwara, Y. Novel Pd(II)- and Pt(II)-Catalyzed Regio- and Stereoselective *trans*-Hydroarylation of Alkynes by Simple Arenes. *J. Am. Chem. Soc.* **2000**, *122* (30), 7252-7263. DOI: 10.1021/ja0005845

(13) The same mechanistic dichotomy exists for the Pd/Pt-catalyzed hydroarylation of alkynes. For recent studies by ^{1}H NMR spectroscopy, mass spectrometry and DFT calculations, see: (a) Godoi, M. N.; de Azambuja, F.; Martinez, P. D. G.; Morgon, N. H.; Santos, V. G.; Regiani, T.; Lesage, D.; Dossmann, H.; Cole, R. B.; Eberlin, M. N.; Correia, C. R. D. Revisiting the Intermolecular Fujiwara Hydroarylation of Alkynes. *Eur. J. Org. Chem.* **2017**, 1794-1803. DOI: 10.1002/ejoc.201700033; (b) Voccia, M.; Falivene, L.; Cavallo, L.; Tubaro, C.; Biffis, A.; Caporaso, L. Ligand Effects in Pd-Catalyzed Intermolecular Alkyne Hydroarylations. *Organometallics* **2019**, *38* (19), 3730-3739. DOI: 10.1021/acs.organomet.9b00473

(14.) Kharasch, M. S.; Isbell, H. S. The chemistry of organic gold compounds. III. Direct introduction of gold into the aromatic nucleus. *J. Am. Chem. Soc.* **1931**, *53* (8), 3053-3059. DOI: 10.1021/ja01359a030

(15) See supporting information for details.

(16) (a) Rocchigiani, L.; Fernandez-Cestau, J.; Agonigi, G.; Chambrier, I.; Budzelaar, P. H. M.; Bochmann, M. Gold(III) Alkyne Complexes: Bonding and Reaction Pathways. *Angew. Chem. Int. Ed.* **2017**, *56* (44), 13861-13865. DOI: 10.1002/anie.201708640; (b) Savjani, N.; Roşca, D.-A.; Schormann, M.; Bochmann, M. Gold(III) Olefin Complexes. *Angew. Chem. Int. Ed.* **2013**, *52* (3), 874-877. DOI: 10.1002/anie.201208356

(17) Kather, R.; Lork, E.; Vogt, M.; Beckmann, J. Stable Borane Adducts of Alcoholates and Carboxylates. *Z. Anorg. Allg. Chem.* **2017**, *643* (10), 636-641. DOI: 10.1002/zaac.201700058

(18) For representative examples of κ^1 and κ^2 OAc^F complexes with Rh and Bi, see: (a) Dikarev, E. V.; Gray, T. G.; Li, B. Heterobimetallic Main-Group–Transition-Metal Paddle-Wheel Carboxylates. *Angew.*

Chem. Int. Ed. **2005**, *44* (11), 1721-1724. DOI: 10.1002/anie.200462433; (b) Feller, M.; Ben-Ari, E.; Gupta, T.; Shimon, L. J. W.; Leitus, G.; Diskin-Posner, Y.; Weiner, L.; Milstein, D. Mononuclear Rh(II) PNP-Type Complexes. Structure and Reactivity. *Inorg. Chem.* **2007**, *46* (25), 10479-10490. DOI: 10.1021/ic701044b; (c) Dikarev, E. V.; Li, B. Rational Syntheses, Structure, and Properties of the First Bismuth(II) Carboxylate. *Inorg. Chem.* **2004**, *43* (11), 3461-3466. DOI: 10.1021/ic049937h; (d) Jurrat, M.; Maggi, L.; Lewis, W.; Ball, L. T. Modular bismacycles for the selective C–H arylation of phenols and naphthols. *Nat. Chem.* **2020**, *12* (3), 260-269. DOI: 10.1038/s41557-020-0425-4

(19) (a) Rodriguez, J.; Szalóki, G.; Sosa Carrizo, E. D.; Saffon-Merceron, N.; Miqueu, K.; Bourissou, D. Gold(III) π-Allyl Complexes. *Angew. Chem. Int. Ed.* **2020**, *59* (4), 1511-1515. DOI: 10.1002/anie.201912314; (b) Rodriguez, J.; Holmsen, M. S. M.; García-Rodeja, Y.; Sosa Carrizo, E. D.; Lavedan, P.; Mallet-Ladeira, S.; Miqueu, K.; Bourissou, D. Nucleophilic Addition to π-Allyl Gold(III) Complexes: Evidence for Direct and Undirect Paths. *J. Am. Chem. Soc.* **2021**, *143* (30), 11568-11581. DOI: 10.1021/jacs.1c04282

(20) Another isomer with the C_{ipso}–H bond pointing towards the OAc^F group (but otherwise very similar in structure and bonding) was found 3.2 kcal/mol higher in energy.[15]

(21) Blons, C.; Amgoune, A.; Bourissou, D. Gold(III) π complexes. *Dalton Trans.* **2018**, *47* (31), 10388-10393. DOI: 10.1039/C8DT01457D

(22) Ghosh, M. K.; Tilset, M.; Venugopal, A.; Heyn, R. H.; Swang, O. Ping-Pong at Gold: Proton Jump Between Coordinated Phenyl and η^1-Benzene Ligands, A Computational Study. *J. Phys. Chem. A* **2010**, *114* (31), 8135-8141. DOI: 10.1021/jp1040508

(23) (a) Rocchigiani, L.; Fernandez-Cestau, J.; Budzelaar, P. H. M.; Bochmann, M. Arene C–H activation by gold(III): solvent-enabled proton shuttling, and observation of a pre-metallation Au–arene intermediate. *Chem. Commun.* **2017**, *53* (31), 4358-4361. DOI: 10.1039/C7CC01628J; (b) Rekhroukh, F.; Blons, C.; Estévez, L.; Mallet-Ladeira, S.; Miqueu, K.; Amgoune, A.; Bourissou, D. Gold(III)–arene complexes by insertion of olefins into gold–aryl bonds. *Chem. Sci.* **2017**, *8* (6), 4539-4545. DOI: 10.1039/C7SC00145B

(24) (a) Heckler, J. E.; Zeller, M.; Hunter, A. D.; Gray, T. G. Geminally Diaurated Gold(I) Aryls from Boronic Acids. *Angew. Chem. Int. Ed.* **2012**, *51* (24), 5924-5928. DOI: 10.1002/anie.201201744; (b) Gómez-Suárez, A.; Dupuy, S.; Slawin, A. M. Z.; Nolan, S. P. Straightforward Synthetic Access to *gem*-Diaurated and Digold σ,π-Acetylide Species. *Angew. Chem. Int. Ed.* **2013**, *52* (3), 938-942. DOI: 10.1002/anie.201208234

(25) (a) Chambrier, I.; Rocchigiani, L.; Hughes, D. L.; Budzelaar, P. H. M.; Bochmann, M. Thermally Stable Gold(III) Alkene and Alkyne Complexes: Synthesis, Structures, and Assessment of the *trans*-Influence on Gold–Ligand Bond Enthalpies. *Chem. Eur. J.* **2018**, *24* (44), 11467-11474. DOI: 10.1002/chem.201802160; (b) Balcells, D.; Eisenstein, O.; Tilset, M.; Nova, A. Coordination and insertion of alkenes and alkynes in Au^{III} complexes: nature of the intermediates from a computational perspective. *Dalton Trans.* **2016**, *45* (13), 5504-5513. DOI: 10.1039/c5dt05014f; (c) Gregori, L; Sorbelli, D.; Belpassi, L.; Tarantelli, F.; Belanzoni, P. Alkyne Activation with Gold(III) Complexes: A Quantitative Assessment of the Ligand Effect by Charge-Displacement Analysis. *Inorg. Chem.* **2019**, *58* (5), 3115-3129. DOI: 10.1021/acs.inorgchem.8b03172

(26) Confirmed by GC analysis upon comparison of the retention time with an authentic sample of the hydroarylation product obtained using Fujiwara's conditions or BCF as cocatalyst.[15]

(27) (a) O'Hair, R. A. J. The 3D quadrupole ion trap mass spectrometer as a complete chemical laboratory for fundamental gas-phase studies of metal mediated chemistry. *Chem. Commun.* **206**, 1469-1481. DOI: 10.1039/B516348J; (b) Santos, L. S. *Reactive Intermediates*. Wiley-VCH, Weinheim, 2010; (c) Schröder, D. Applications of Electrospray Ionization Mass Spectrometry in Mechanistic Studies and Catalysis Research. *Acc. Chem. Res.* **2012**, *45* (9), 1521-1532. DOI: 10.1021/ar3000426; (d) Mehara, J.; Roithová, J. Identifying reactive intermediates by mass spectrometry. *Chem. Sci.* **2020**, *11* (44), 11960-11972. DOI: 10.1039/d0sc04754f

(28) Serra, J.; Font, P.; Sosa Carrizo, E. D.; Mallet-Ladeira, S.; Massou, S.; Parella, T.; Miqueu, K.; Amgoune, A.; Ribas, X.; Bourissou, D. Cyclometalated gold(III) complexes: noticeable differences between (N,C) and (P,C) ligands in migratory insertion. *Chem. Sci.* **2018**, *9* (16), 3932-3940. DOI: 10.1039/C7SC04899H

(29) Sabatelli, F.; Segato, J.; Belpassi, L.; Del Zotto, A.; Zuccaccia, D.; Belanzoni, P. Monitoring of the Pre-Equilibrium Step in the Alkyne Hydration Reaction Catalyzed by Au(III) Complexes: A Computational Study Based on Experimental Evidences. *Molecules* **2021**, *26* (9), 2445. DOI: 10.3390/molecules26092445

(30) Wang, W.; Hammond, G. B.; Xu, B. Ligand Effects and Ligand Design in Homogeneous Gold(I) Catalysis. *J. Am. Chem. Soc.* **2012**, *134* (12), 5697-5705. DOI: 10.1021/ja3011397

(31) The following trend has been established experimentally for the kinetic basicity of organogold compounds: sp^3 < sp < sp^2: Roth, K. E.; Blum, S. A. Relative Kinetic Basicities of Organogold Compounds. *Organometallics* **2010**, *29* (7), 1712-1716. DOI: 10.1021/om901101f

(32) (a) Ciancaleoni, G.; Belpassi, L.; Zuccaccia, D.; Tarantelli, F.; Belanzoni, P. Counterion Effect in the Reaction Mechanism of NHC Gold(I)-Catalyzed Alkoxylation of Alkynes: Computational Insight into Experiment. *ACS Catal.* **2015**, *5* (2), 803-814. DOI: 10.1021/cs501681f; (b) Gaggioli, C. A.; Ciancaleoni, G.; Zuccaccia, D.; Bistoni, G.; Belpassi, L.; Tarantelli, F.; Belanzoni, P. Strong Electron-Donating Ligands Accelerate the Protodeauration Step in Gold(I)-Catalyzed Reactions: A Quantitative Understanding of the Ligand Effect. *Organometallics* **2016**, *35* (13), 2275-2285. DOI: 10.1021/acs.organomet.6b00346; (c) BabaAhmadi, R.; Ghanbari, P.; Rajabi, N. A.; Hashmi, A. S. K.; Yates, B. F.; Ariafard, A. A Theoretical Study on the Protodeauration Step of the Gold(I)-Catalyzed Organic Reactions. *Organometallics* **2015**, *34* (13), 3186-3195. DOI: 10.1021/acs.organomet.5b00219

(33) Wang, W.; Kumar, M.; Hammond, G. B.; Xu, B. Enhanced Reactivity in Homogeneous Gold Catalysis through Hydrogen Bonding. *Org. Lett.* **2014**, *16* (2), 636-639. DOI: 10.1021/ol403584e